

Equilibrium models of radially anisotropic spherical stellar systems with softened central potentials

E. V. Polyachenko,^{1*}, V. L. Polyachenko,¹ I. G. Shukhman,^{2†}

¹*Institute of Astronomy, Russian Academy of Sciences, 48 Pyatnitskaya St., Moscow 119017, Russia*

²*Institute of Solar-Terrestrial Physics, Russian Academy of Sciences, Siberian Branch, P.O. Box 291, Irkutsk 664033, Russia*

Accepted Received

ABSTRACT

We study a new class of equilibrium two-parametric distribution functions of spherical stellar systems with radially anisotropic velocity distribution of stars. The models are less singular counterparts of the so called generalized polytropes, widely used in works on equilibrium and stability of gravitating systems in the past. The offered models, unlike the generalized polytropes, have finite density and potential in the center. The absence of the singularity is necessary for proper consideration of the radial orbit instability, which is the most important instability in spherical stellar systems. Comparison of the main observed parameters (potential, density, anisotropy) predicted by the present models and other popular equilibrium models is provided.

Key words: Galaxy: center, galaxies: kinematics and dynamics.

1 INTRODUCTION

Equilibrium models of spherical stellar systems are needed for observations and numerical simulations of open and globular clusters (see, e.g. Kharchenko et al. 2009, Ernst & Just 2013). On the other hand, our interest in developing a new class of radially-anisotropic models is explained by our desire to perform correct stability analysis of systems with nearly radial orbits. The gravitational potential and radial force in models of spherical stellar systems in which all stars travel on purely radial orbits are singular. This makes it impossible to apply the standard methods of the linear stability theory, and also cast doubts on some of the works on Radial Orbits Instability (ROI) (see e.g. Antonov, 1973).

Even a small dispersion in the angular momentum can improve the situation, however, its presence cannot guarantee the removal of the singularity. An example is a series of models known as generalized polytropes, which remain singular despite having some dispersion (see, e.g., Bisnovatyi-Kogan and Zel'dovich, 1969; Hénon, 1973). The potential at $r \approx 0$ determines the behavior of the precession rate Ω_{pr} at small angular momentum, which plays a significant role in the stability of the system (Polyachenko et al. 2010). For singular potentials, the precession rate is no longer proportional to the angular momentum, and very quickly (with infinite derivative) departs from zero for angular momentum near $L = 0$ (see, e.g., Touma and Tremaine, 1997). In this case, usual arguments concerning the mechanism of radial orbit

instability which, in particular, involve the linear approximation for the precession rate (see, e.g., Palmer 1994) are not useful.

Note that most works that include spectrum determination by matrix methods use models that cannot be made arbitrarily close to systems with purely radial orbits. The standard choice is Osipkov-Merritt type DFs (Osipkov, 1979; Merritt 1985). However, these DFs have restrictions on the largest possible radial anisotropy.

The simplest isotropic self-gravitating polytrope $F(E) \propto (-2E)^q$, where $E = \frac{1}{2}(v_r^2 + v_\perp^2) + \Phi(r) \leq 0$ is the energy (see, e.g., Fridman & Polyachenko 1984) can be used to construct a series of purely radial models

$$F(E) \propto \delta(L^2)(-2E)^q, \quad (1.1)$$

where $\delta(x)$ is the Dirac delta-function, $L = r v_\perp$ is the absolute value of the angular momentum of a star. Generalization of (1.1) is possible by replacing the delta-functions on the distribution of the form

$$\delta(L^2) \rightarrow \frac{H(L_T^2 - L^2)}{L_T^2},$$

where $H(x)$ is the Heaviside step function. In the limit $L_T \rightarrow 0$ the function $H(L_T^2 - L^2)/L_T^2$ becomes the delta-function,

$$\int \frac{d(L^2)}{L_T^2} H(L_T^2 - L^2) = 1, \quad \lim_{L_T \rightarrow 0} \frac{H(L_T^2 - L^2)}{L_T^2} = \delta(L^2).$$

The allowed range of parameter q coincides with the range of the polytropic index in classical polytropic models: $-1 \leq q < \frac{7}{2}$ (see, e.g., Binney & Tremaine, 2008). Parameter L_T specifies width of the phase space region over angular momentum L occupied by the model, $L_T \geq 0$. If L_T

* E-mail: epolyach@inasan.ru

† E-mail: shukhman@iszf.irk.ru

is less than some critical value $(L_T)_{\text{iso}}(q)$ then radial motions dominate. $(L_T)_{\text{iso}}(q)$ has the meaning of the maximum specific angular momentum of the particles in an isotropic self-gravitating polytrope of index q . For $L_T \geq (L_T)_{\text{iso}}(q)$ models no longer depend on L_T and become isotropic.

In contrast with the previously used models, the proposed anisotropic polytropes reach the limit of purely radial systems for a wide region of polytropic index q . Besides, relative simplicity of the models allows one to achieve good accuracy for eigenmodes and stability boundaries, which in turn can help in understanding the mechanism of ROI.

In Sec. 2 we give general equations and provide profiles of the potential, density, and anisotropy for the proposed models, and for several other models commonly used for spherical systems. Sec. 3 is devoted to the study properties of the models in the limit $L_T = 0$. Then, in Sec. 4 we explore in more details several special families of models for which the equilibrium state can be obtained analytically or stability analysis is particularly simple. Sec. 5 stresses on the orbit's precession behavior of nearly radial orbits, and on difficulties that arise in systems with purely radial orbits. In Sec. 6 we summarize the results.

2 SOFTENED ANISOTROPIC POLYTROPES

In this paper we consider two-parametric series (parameters q and L_T) of models with DF

$$F(E, L) = \frac{N}{4\pi^3 L_T^2} H(L_T^2 - L^2) F_0(E),$$

where $N = N(q, L_T)$ is a constant defined by the normalization condition that the total mass of the system $M = 1$. For simplicity, we assume that the gravitational constant and a radius of the spherical system are equal to unity as well: $G = 1$, $R = 1$. Dependence of the DF on energy is supposed to be the same as in the classical polytropic models,

$$F_0(E) = 2(1+q)(-2E)^q. \quad (2.1)$$

The form of (2.1) suggests that an additive constant in the potential $\Phi_0(r)$ is chosen in such a way that the potential is equal to zero on the sphere boundary, $\Phi_0(1) = 0$. Moreover, the factor $(q+1)$ allows to include the boundary value $q = -1$ in the region of available values, since $\lim_{q \rightarrow -1^+} F_0(E) = \delta(E)$ (see, e.g., Gelfand and Shilov, 1964).

Then, it is convenient to define the relative potential and the relative energy of a star by $\Psi(r) = -\Phi_0(r) \geq 0$, $\mathcal{E} = -E \geq 0$, and use the DF in the form:

$$F(\mathcal{E}, L) = \frac{N(q, L_T)(1+q)}{2\pi^3 L_T^2} H(L_T^2 - L^2) (2\mathcal{E})^q. \quad (2.2)$$

Below, we shall refer to this models as ‘‘softened’’ anisotropic polytropes or PPS polytropes.

For density distribution one obtains:

$$\rho(r) = \frac{N}{\pi^2 L_T^2} \frac{\Gamma(q+2)\Gamma(\frac{3}{2})}{\Gamma(q+\frac{5}{2})} (2\Psi)^{q+3/2} \times \begin{cases} 1 & \text{for } 2\Psi r^2 < L_T^2, \\ 1 - [1 - L_T^2/(2\Psi r^2)]^{q+3/2} & \text{for } 2\Psi r^2 > L_T^2. \end{cases} \quad (2.3)$$

Here $\Gamma(z)$ denotes the Gamma function. With a newly defined function,

$$\mathcal{F}_n(x) = 1 - [1 - \min(1, x)]^n,$$

the expression for density can be written in the compact form,

$$\rho = A (2\Psi)^{q+3/2} \mathcal{F}_{q+\frac{3}{2}}\left(\frac{L_T^2}{2r^2\Psi}\right), \quad (2.4)$$

where

$$A \equiv \frac{N}{\pi^2 L_T^2} \frac{\Gamma(q+2)\Gamma(\frac{3}{2})}{\Gamma(q+\frac{5}{2})}.$$

The number of solutions of equation

$$2r^2\Psi(r) = L_T^2 \quad (2.5)$$

depends on the value of L_T^2 . Given L_T is less than the maximum specific angular momentum in the isotropic polytrope,

$$(L_T)_{\text{iso}}(q) = \max_r [2r^2\Psi(r)]^{1/2} = L_{\text{circ}}(0),$$

where $L_{\text{circ}}(0)$ is the specific angular momentum of the star with $\mathcal{E} = 0$ in a circular orbit in the polytrope q , equation (2.5) has two solutions $0 < r_1 < r_2 < 1$. A condition $2r^2\Psi < L_T^2$ is satisfied in the regions adjacent to the center, $0 \leq r < r_1$, and to the boundary of the sphere, $r_2 < r \leq 1$ (regions I and III respectively). In the region II ($r_1 < r < r_2$), $2r^2\Psi > L_T^2$. The dependence of $(L_T)_{\text{iso}}(q)$ is given in Fig. 10a in Sec. 6.

For $L_T \ll 1$, the solutions r_1, r_2 tend to 0 and 1, consequently. Since $\Psi(r_1) \simeq \Psi(0) + \mathcal{O}(r_1^2)$, $r_1 \simeq L_T/\sqrt{2\Psi(0)}$. Similarly, $\Psi(r_2) \simeq -(1-r_2)\Psi'(1) + \mathcal{O}[(1-r_2)^2]$, so $1-r_2 \simeq L_T^2/[-2\Psi'(1)] = L_T^2/2$. Here $\Psi'(1) = -GM/R^2 = -1$ from $G = R = M = 1$.

The Poisson equation

$$\Psi'' + \frac{2}{r}\Psi' = -4\pi\rho(r) \quad (2.6)$$

together with boundary conditions:

$$\Psi'(0) = 0, \quad \Psi(1) = 0, \quad \Psi'(1) = -1 \quad (2.7)$$

determine the potential Ψ and the normalization constant $N = N(q, L_T)$.

Generally, equation (2.6) with boundary conditions (2.7) is solved numerically. However, several values of q result in analytic solutions. As is the case for isotropic polytropes, if $L_T > (L_T)_{\text{iso}}$, analytic solutions exist for $q = -\frac{3}{2}, -\frac{1}{2}, \frac{7}{2}$. However, if $q < -1$, the distribution is unphysical (i.e. unintegrable) and the $q = -\frac{3}{2}$ case is thus unphysical. The $q = \frac{7}{2}$ case, which corresponds to the Plummer model, on the other hand results in solutions with infinite radius, which is also must be rejected due to the boundary condition. In fact the finite radius condition restricts $q < \frac{7}{2}$. In the $L_T = 0$ limit, analytical solutions are found for $q = -\frac{1}{2}, \frac{1}{2}$, but the $q = \frac{1}{2}$ case leads to no physically acceptable solutions with finite radius. Connecting two limits, for arbitrary L_T , the equation has exact analytical solutions if $q = -\frac{1}{2}$, for which the source term of the equation becomes linear on Ψ . In addition, if $q = 1/2$, equation (2.6) for region II, where $2\Psi r^2 > L_T^2$, is analytically solvable. Hence, in the $q = \frac{1}{2}$ case it is possible to construct approximate analytic physically acceptable solutions with finite mass and radius, if $L_T > 0$. The solutions for $L_T \ll 1$, which ignore narrow region III (with width $\propto L_T^2$), are constructed in Appendix.

Fig. 1 illustrates a comparison of the potential and the density for our model (2.2) at $q = \frac{1}{2}$, $L_T \simeq 0.2$ with the corresponding profiles obtained for the generalized polytropes (hereafter GP) (see, e.g., Polyachenko et al., 2011):

$$F_{\text{GP}}(\mathcal{E}, L) = C(s, q) L^{-s} (2\mathcal{E})^q, \quad (2.8)$$

and for Osipkov-Merritt (hereafter OM) models of type

$$F_{\text{OM}}(\mathcal{E}, L) = A(r_a, p) Q^p, \quad Q = \mathcal{E} - \frac{1}{2} L^2 / r_a^2, \quad (2.9)$$

where A is a normalization constant and r_a is the so called anisotropy radius (Osipkov, 1979; Merritt, 1985).

Parameters of GP and OM models have been selected in such a way that the global anisotropy (2.12) (see below for the definition) in all the models was the same and equal to $\xi \simeq 0.65$, that roughly corresponded to the predominance of the total radial kinetic energy of stars over the total transversal kinetic energy by factor of 3/2. A certain degree of freedom in choosing the parameters r_a and p for the OM DFs were used to fit the potential and density profiles of the PPS polytrope.

Curves of the potentials for different models almost coincide at $r > r_1 \approx 0.070$. Difference is noticeable in the central region $r < r_1$, where PPS polytropes become isotropic. However, distribution of density is significantly different: while PPS polytropes and OM models demonstrate similar behavior and finite density in the center, the generalized polytropic models show rather strong singularity, $\rho \sim r^{-s}$.

The *local* anisotropy parameter (see, e.g., Binney & Tremain, 2008)

$$\beta(r) \equiv 1 - \frac{1}{2} \langle v_{\perp}^2 \rangle / \langle v_r^2 \rangle, \quad (2.10)$$

is an important characteristics of stellar systems. Here $\langle v_r^2 \rangle$ and $\langle v_{\perp}^2 \rangle$ are dispersions of radial and transversal velocities respectively:

$$\begin{aligned} \langle v_r^2 \rangle &= \frac{2\pi}{r^3 \rho(r)} \int v_r^2 v_{\perp} dv_{\perp} dv_r F(\mathcal{E}, L) \\ &= \frac{2\pi}{r^3 \rho(r)} \int d\mathcal{E} dL^2 F(\mathcal{E}, L) (L_{\text{max}}^2 - L^2)^{1/2}, \end{aligned}$$

$$\begin{aligned} \langle v_{\perp}^2 \rangle &= \frac{2\pi}{\rho(r)} \int v_{\perp}^3 dv_{\perp} dv_r F(\mathcal{E}, L) \\ &= \frac{2\pi}{r^3 \rho(r)} \int d\mathcal{E} dL^2 F(\mathcal{E}, L) L^2 (L_{\text{max}}^2 - L^2)^{-1/2}, \end{aligned}$$

where $L_{\text{max}}(r, \mathcal{E}) \equiv \sqrt{2r^2 [\Psi(r) - \mathcal{E}]}$. Either by direct integration of the DF or using the method of Dejonghe (1986) (see also Dejonghe & Merritt, 1992) one obtains for PPS polytropes

$$\rho(v_r^2) = \frac{A}{2q+5} (2\Psi)^{q+5/2} \mathcal{F}_{q+5/2},$$

and

$$\rho(v_{\perp}^2) = 2\Psi\rho - (2q+3)\rho(v_r^2), \quad (2.11)$$

and so

$$\beta = (q + \frac{5}{2})(1 - \mathcal{F}_{q+3/2}/\mathcal{F}_{q+5/2}).$$

Profiles of local anisotropy are shown in Fig. 2. In the central region I ($r < r_1$) PPS polytrope is isotropic ($\beta = 0$), while beyond this radius (region II, $r_1 < r$) it quickly becomes radially-anisotropic, $\beta > 0$. Note that in contrast with OM models, anisotropy profiles for PPS polytropes

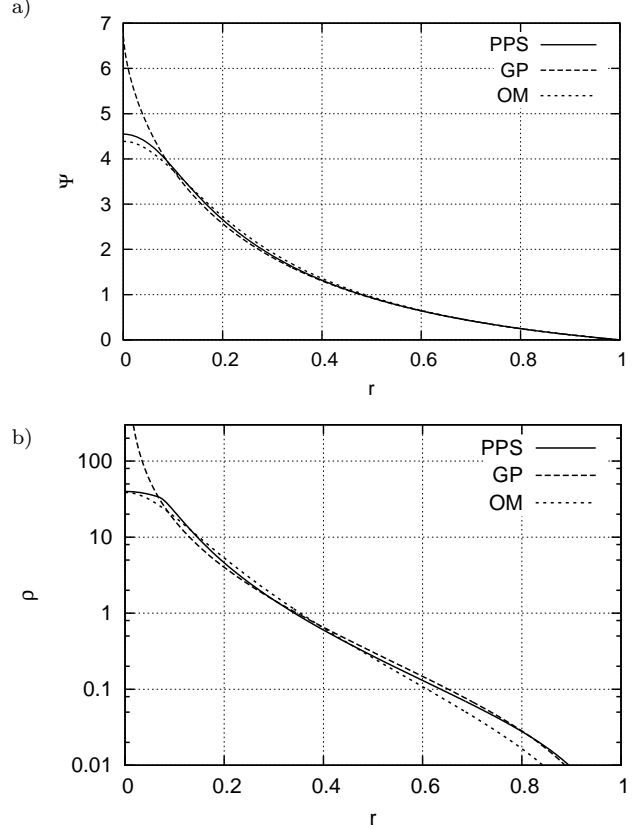


Figure 1. (a) Potential $\Psi(r)$ and (b) density $\rho(r)$ for PPS polytrope, GP for $q = \frac{1}{2}$, and OM model for $p = -1/8$, $r_a = 0.12$. Other parameters of the first two models ($L_T \simeq 0.2$, $s \simeq 1.3$) were chosen so that global anisotropy for all models was identical, $\xi \simeq 0.65$. For PPS polytrope, $r_1 \approx 0.070$, $r_2 \approx 0.979$.

are non-monotonic. Near the boundary of sphere (region III, $r_2 < r < 1$) the velocity distribution again becomes isotropic, and $\beta(r)$ decreases sharply to zero. Experiments with different values of q show that lower q give sharper changes of the anisotropy parameter at boundaries of regions I-II and II-III, although in general behavior of $\beta(r)$ changes insignificantly. The anisotropy parameter for generalized polytropes does not depend on radius, $\beta = \frac{1}{2} s$.

A system as a whole can be characterized by the parameter of *global* anisotropy $\zeta \equiv 2T_r/T_{\perp}$ (Fridman & Polyachenko, 1984), where $T_r = 4\pi \int_0^1 dr r^2 \rho(r) \cdot \frac{1}{2} \langle v_r^2 \rangle$ and $T_{\perp} = 4\pi \int_0^1 dr r^2 \rho(r) \cdot \frac{1}{2} \langle v_{\perp}^2 \rangle$ are total radial and transversal kinetic energy of all stars in the system. It is convenient to redefine the anisotropy parameter as follows:

$$\xi(q, L_T) \equiv 1 - \frac{1}{2} T_{\perp}/T_r = 1 - \zeta^{-1}. \quad (2.12)$$

Then $\xi = 0$ corresponds to isotropic systems (in average), while $\xi = 1$ implies purely radial systems. Thus, the definition of ξ is consistent with the definition of the local parameter β and we shall use it henceforth as a global characteristics for stellar models.

Comparison of global anisotropy for PPS polytropes and OM model is shown in Fig. 3. A characteristic feature of OM model is that for any parameters p and r_a , the value of the global anisotropy does not reach unity. In contrast, in the PPS polytropes the limit of purely radial systems exists for a wide range of parameters q : $-1 \leq q < \frac{1}{2}$. This is es-

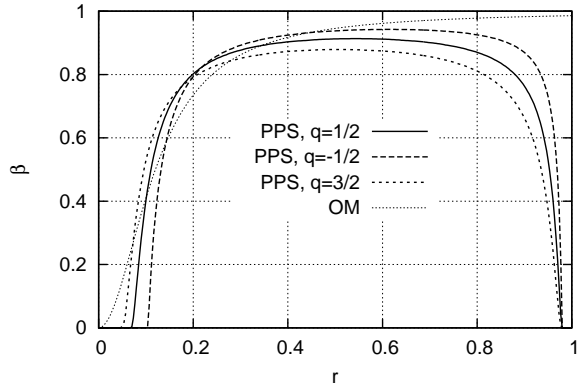


Figure 2. Radial dependence of the local anisotropy $\beta(r)$ for PPS polytrope, and for OM model, $\beta(r) = (1 + r_a^2/r^2)^{-1}$, for several values of q . Parameters of models are the same as in Fig. 1. The local anisotropy for classical GP is constant, $\beta \simeq 0.65$ (not shown).

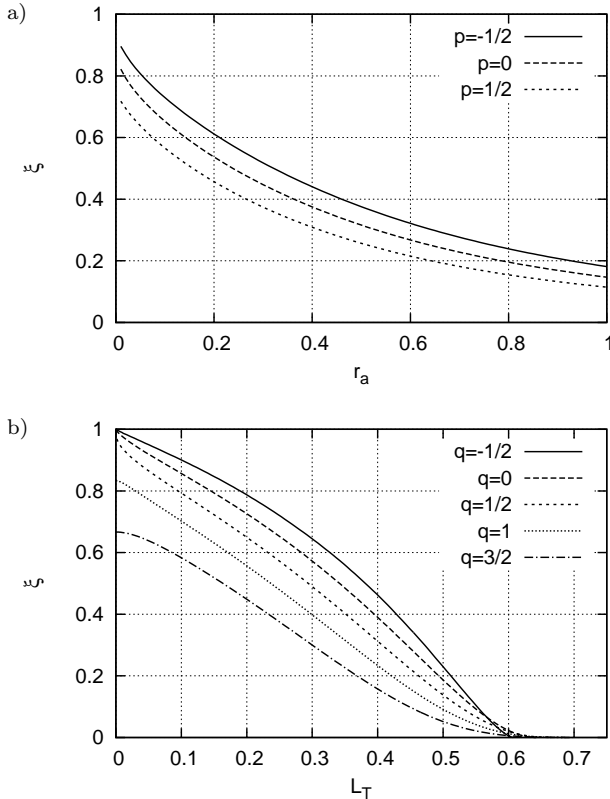


Figure 3. Dependence of global anisotropy (a) for OM model v.s. parameter r_a for $p = -\frac{1}{2}, 0, \frac{1}{2}$, and (b) for PPS polytrope v.s. parameter L_T for $q = -\frac{1}{2}, 0, \frac{1}{2}, 1, \frac{3}{2}$.

essential for further study of stability of systems with nearly radial orbits. Properties of models near purely radial orbits boundary $L_T = 0$ are considered in the next section in more details.

For PPS polytropes, from $\langle v_\perp^2 \rangle + (2q+3)\langle v_r^2 \rangle = 2\Psi$ (see

(2.11), one also obtains

$$T_\perp + (2q+3)T_r = 4\pi \int_0^R dr r^2 \rho \Psi,$$

or

$$T_\perp + (2q+3)T_r = -\frac{GM^2}{R} - 2W, \quad (2.13)$$

where W is the total potential energy of a self-gravitating system

$$W = 4\pi \int_0^R dr r^2 \cdot \frac{1}{2} \rho \Phi, \quad (2.14)$$

and Φ is the potential with the zero point given $\Phi(\infty) = 0$; $\Psi = \Phi(R) - \Phi(r) = -GM/R - \Phi$. Together with the virial theorem, $2(T_\perp + T_r) + W = 0$ and definition of global anisotropy parameter (2.12), this means that one can express the total kinetic and potential energy via q and ξ ,

$$\begin{bmatrix} 2q+3 & 1 & 2 \\ 2 & 2 & 1 \\ 2(1-\xi) & -1 & 0 \end{bmatrix} \begin{bmatrix} T_r \\ T_\perp \\ W \end{bmatrix} = \begin{bmatrix} -GM^2/R \\ 0 \\ 0 \end{bmatrix}. \quad (2.15)$$

Provided that $\Delta \equiv 7 - 2q - 6\xi \neq 0$,

$$T_r = \frac{1}{\Delta} \frac{GM^2}{R}, \quad T_\perp = \frac{2(1-\xi)}{\Delta} \frac{GM^2}{R},$$

$$W = -\frac{2(3-2\xi)}{\Delta} \frac{GM^2}{R}. \quad (2.16)$$

Alternatively, at fixed q , the global anisotropy of PPS polytropes is related to the potential energy:

$$\xi = \frac{(\frac{7}{2} - q)w - 3}{3w - 2}, \quad (2.17)$$

where $w \equiv \frac{|W|}{GM^2/R} = -\frac{W}{GM^2/R}$.

3 SOFTENED ANISOTROPIC POLYTROPES AT $L_T \rightarrow 0$

Specifics of radial and nearly radial systems is a central singularity, and therefore they require special consideration. The GP models (2.8) give purely radial orbits at $s = 2$. However, not every q is allowed: as it was noted by Hénon (1973) and Barnes et al. (1986), no GP exists when $2q + 3s \geq 7$. Thus, GPs provide systems consisting of radial orbits only when $q < 1/2$. This also can be seen from our model equations provided that $L_T = 0$. Substituting density

$$\rho(r) = \frac{N}{2\pi^2} \frac{\Gamma(q+2)\Gamma(\frac{1}{2})}{\Gamma(q+\frac{3}{2})} \frac{(2\Psi)^{q+1/2}}{r^2}$$

into the Poisson equation and using $x \equiv \ln(1/r)$ as a new independent variable one obtains

$$\frac{d^2\Psi}{dx^2} - \frac{d\Psi}{dx} = -D(2\Psi)^{q+1/2}, \quad (3.1)$$

$$D \equiv \frac{2N}{\pi} \frac{\Gamma(q+2)\Gamma(\frac{1}{2})}{\Gamma(q+\frac{3}{2})}. \quad (3.2)$$

An asymptotic solution for $x \rightarrow \infty$ (or for $r \rightarrow 0$) is

$$\Psi(x) \propto x^m, \quad m = (\frac{1}{2} - q)^{-1} > 0, \quad (3.3)$$

from where we infer that such solutions are possible for $q < \frac{1}{2}$ only.

For $q = \frac{1}{2}$, equation (3.1) becomes linear and has exact analytical solutions. Unfortunately, from its two linearly independent solutions it is impossible to construct a solution which would have a finite mass and finite potential energy. However, if we admit arbitrarily small smearing, $L_T \neq 0$, a solution with a finite radius is possible (see Appendix for details).

The models with purely radial orbits are always singular, and the singularity is not weaker than $\rho \propto r^{-2}$. This was first pointed out by Bouvier & Janin (1968) (see also Richstone & Tremaine, 1984). However, it is more accurate to say that the singularity may be slightly stronger or slightly weaker than r^{-2} : $\rho(r) \propto r^{-2}[\Psi(r)]^{1/2+q}$. Since $\Psi(r) \propto [\ln(1/r)]^m$ with positive m [see (3.3)] one obtains that, for $q < -\frac{1}{2}$ the singularity is slightly weaker than r^{-2} .

In the limit of $L_T \rightarrow 0^+$, asymptotic solution for $q > \frac{1}{2}$ takes the form $\Psi(x) \propto \exp(x) = 1/r - 1$, i.e. models degenerate into a point (considering the adopted length unit). The normalization constant in this case tends to zero: $N(q, L_T) \propto L_T^{2q-1}$ at $L_T \rightarrow 0$. Global anisotropy ξ for these models is less than one, which is evident, e.g., from Fig. 3b. It may seem that there is a contradiction: on one hand the parameter L_T tends to zero, and on the other hand the parameter ξ , which characterizes the anisotropy of the system as a whole, tends to a finite limit less than one. In reality, of course, there is no contradiction. With an increase of polytropic index q the number of particles with energy $E \sim 0$ decreases, and the particles with energies close to the minimum potential energy begin to dominate. For small L_T , the potential well near the center is very deep, so the mass is concentrated near the center in a very small region of $r \lesssim O(L_T^2)$. Outside this region, the potential is actually Keplerian, $\Psi(r) = 1/r - 1$. In fact, radius $r = 1$ is infinitely remote from the region of localization of the mass.

To determine the shape of orbits trapped in this region, one should not rely only on the smallness of the angular momentum in units $(GMR)^{1/2}$. For highly elongated orbits, the angular momentum L should be small compared to an angular momentum of a circular orbit of the same energy $L_{\text{circ}}(E)$, i.e. $L/L_{\text{circ}}(E) \ll 1$. In other words, when L_T is small compared to one, orbits must not be nearly radial, and anisotropy parameter ξ is not required to be close to unity.

To illustrate this we define a localization radius r_{LOC} by the equation

$$\left[\frac{d \ln \rho(r)}{d \ln(1/r)} \right]_{r=r_{\text{LOC}}} = 3, \quad (3.4)$$

which is the radius where the density begins to decrease more rapidly than r^{-3} . The reason is that beyond this radius the gravitational force is determined primarily by the mass confined within r_{LOC} . From Fig. 4 it is seen that models with $q = 0.7$ (fifth curve from above given by heavy solid line) tend to its asymptotics $r_{\text{LOC}} \propto L_T^2$ already for $L_T \sim 10^{-5}$. In fact, this behavior occurs for all values of $q > 0.5$, but in order to demonstrate this, we must consider L_T orders of magnitude less than $L_T \sim 10^{-5}$, which is difficult to implement numerically.

For $L_T \rightarrow 0^+$, the global anisotropy ξ as a function of q can be obtained analytically, if $q > \frac{1}{2}$. The Keplerian potential of the system corresponds to a point mass, if the

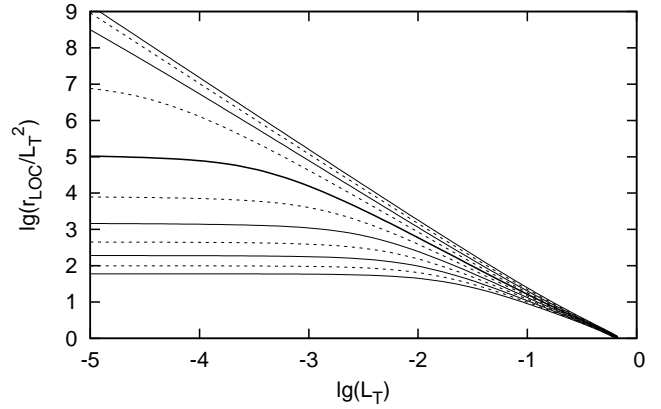


Figure 4. Dependence of localization radius r_{LOC} on L_T at $q > \frac{1}{2}$. Eleven curves are shown, starting from $q = 0.5$ with step 0.05 (from top to bottom). It is seen, that beginning from the fifth curve ($q = 0.7$, heavy solid line) the curves $r_{\text{LOC}}(q, L_T)/L_T^2$ tend to constant values for $L_T \lesssim 10^{-5}$.

outer boundary R is finite. On the other hand, if the system is scaled so that the potential in the center is finite, then $R \rightarrow \infty$, and ‘surface term’ GM^2/R in (2.16) and (2.17) becomes zero. Since all energies cannot all together vanish, it requires the determinant $\Delta = 0$, i.e.

$$\xi = \frac{1}{3} \left(\frac{7}{2} - q \right). \quad (3.5)$$

We see that when parameter q varies from $\frac{1}{2}$ to $\frac{7}{2}$ the models are transformed from a model with purely radial orbits to an isotropic one with $\xi = 0$.

Note that for $q \rightarrow \frac{7}{2}$, the equation (2.6) reduces to the Lane-Emden equation for any finite value $L_T \gg \delta^{1/2}$, where $\delta \equiv \frac{7}{2} - q \ll 1$. Indeed, introducing variables $\Psi = \psi/\delta$, $r = z\delta$, $N = n_0 \delta^2 L_T^2$, we can express (2.6) in the form

$$\frac{d^2 \psi}{dz^2} + \frac{2}{z} \frac{d\psi}{dz} = -\frac{63}{4} n_0 \psi^5 \mathcal{F}_5 \left(\frac{L_T^2}{2\delta \psi z^2} \right)$$

with boundary conditions:

$$\psi(1/\delta) = 0, \quad \psi'(1/\delta) = -\delta^2, \quad \psi'(0) = 0$$

which can be replaced by homogeneous boundary conditions at the origin and at infinity. Point z_1 at which $2\psi(z_1)z_1^2 \approx 2z_1 = L_T^2/\delta$ also goes to infinity, provided that $L_T^2/\delta \gg 1$. The result is the Lane-Emden equation

$$\psi'' + \frac{2}{z} \psi' = -\frac{63}{4} n_0 \psi^5$$

the solution of which gives the well-known Plummer potential $\psi = (a^2 + z^2)^{-1/2}$ with $a = \sqrt{\frac{21}{4}} n_0$, which corresponds to the isotropic polytropic model with $q = \frac{7}{2}$. Our calculations give $n_0 \approx 0.00183$, i.e. $a \approx 0.098$.

4 SPECIAL FAMILIES

Here we consider several special families of PPS polytropes for which the equilibrium state can be obtained analytically or stability analysis is particularly simple: $q = \frac{1}{2}$, $q = 0$, $q = -\frac{1}{2}$, $q = -1$.

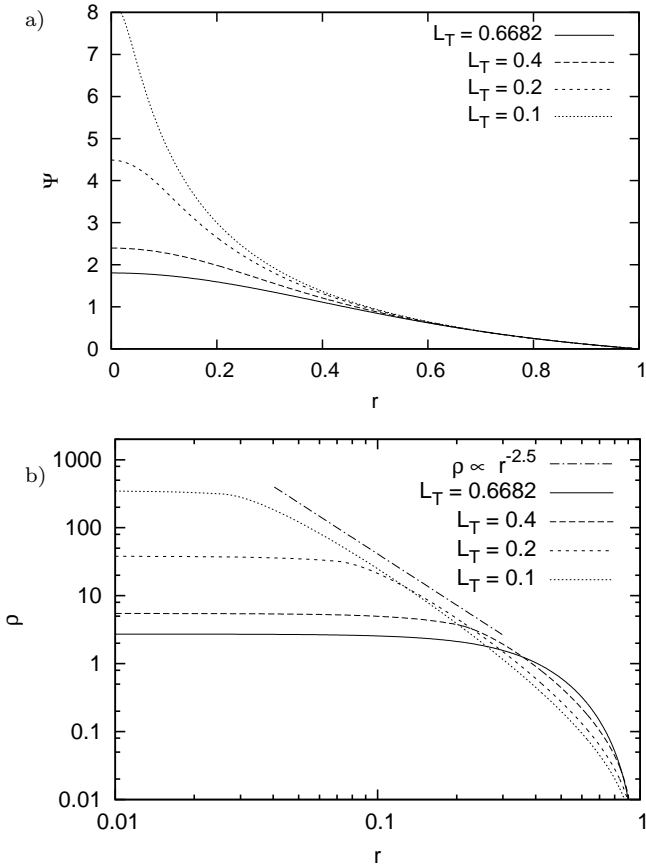


Figure 5. (a) The potential profiles and (b) the density profiles for models with $q = \frac{1}{2}$ and several values of L_T . The maximum value of L_T plotted corresponds to $(L_T)_{\text{iso}}(q)$ and so the corresponding model is identical to the isotropic polytrope of index q . The dash-dotted line shows the density slope $\rho \propto r^{-2.5}$.

4.1 Models with $q = \frac{1}{2}$

The model with a DF

$$F(E, L) = \frac{3N}{4\pi^3} \frac{H(L_T^2 - L^2)}{L_T^2} \sqrt{-2E}$$

is a boundary model, which in the limit $L_T \rightarrow 0^+$ is turned into purely radial one, i.e. $\xi(\frac{1}{2}, 0^+) = 1$, see Fig. 3b.

Designation “0⁺” emphasizes the already mentioned fact that for $q = \frac{1}{2}$ there is no physically acceptable model with a purely radial orbits, although models with arbitrarily small but finite angular momentum dispersion are possible. Solving the Poisson equation (2.6) with density given by (2.3), it is possible to obtain potential and density profiles for different L_T in the range $0 < L_T < 0.6682$ (see Fig. 5). It turns out that for small values L_T it is possible even to obtain analytical expressions for the potential, density and the normalization constant N . The details of this solution are described in Appendix.

4.2 “Step” models, $q = 0$

The simplest anisotropic model allowing both energy and angular momentum to vary in finite intervals corresponds

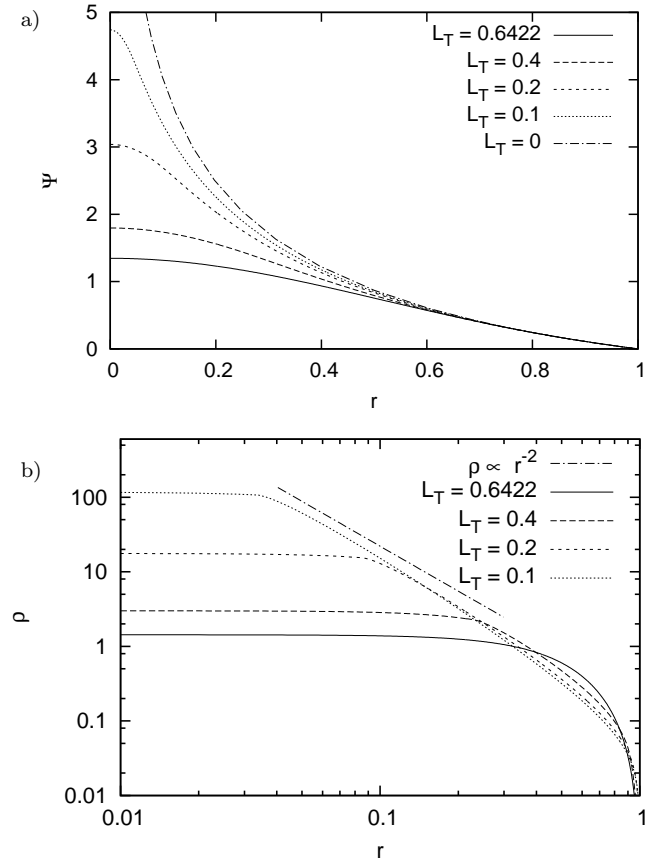


Figure 6. Same as in Fig. 5 for $q = 0$. The dash-dotted line shows the density slope $\rho \propto r^{-2}$.

to parameter $q = 0$:

$$F(E, L) = \frac{N}{2\pi^3} \frac{H(L_T^2 - L^2)}{L_T^2} H(-2E).$$

Study of the stability of such a DF is the simplest, and at the same time, the model is quite realistic.

Solving the Poisson equation (2.6) it is possible to obtain profiles of the potential and density for different values of L_T in the range $0 < L_T < 0.6422$ (see the Fig. 6).

Fig. 6b demonstrates transformation of density profiles with decreasing L_T . The model with purely radial orbits has a cuspy profile $\rho \sim \ln(1/r)/r^2$. Density profiles of nearly radial models differ from the cuspy profile only in a small region near the center $r < r_1 \sim L_T$.

Dependence of global anisotropy $\xi(L_T)$ for this model is presented in Fig. 3. It is seen, that the limit $L_T \rightarrow 0$ exists and the global anisotropy tends to one.

4.3 Models with $q = -\frac{1}{2}$

This anisotropic model is of interest since it allows the exact analytical solution of the Poisson equation. For $q = -\frac{1}{2}$, the expression for density can be simplified

$$\rho(r) = \frac{N}{4\pi L_T^2} \begin{cases} 2\Psi & \text{for } 2\Psi r^2 < L_T^2, \\ L_T^2/r^2 & \text{for } 2\Psi r^2 > L_T^2. \end{cases}$$

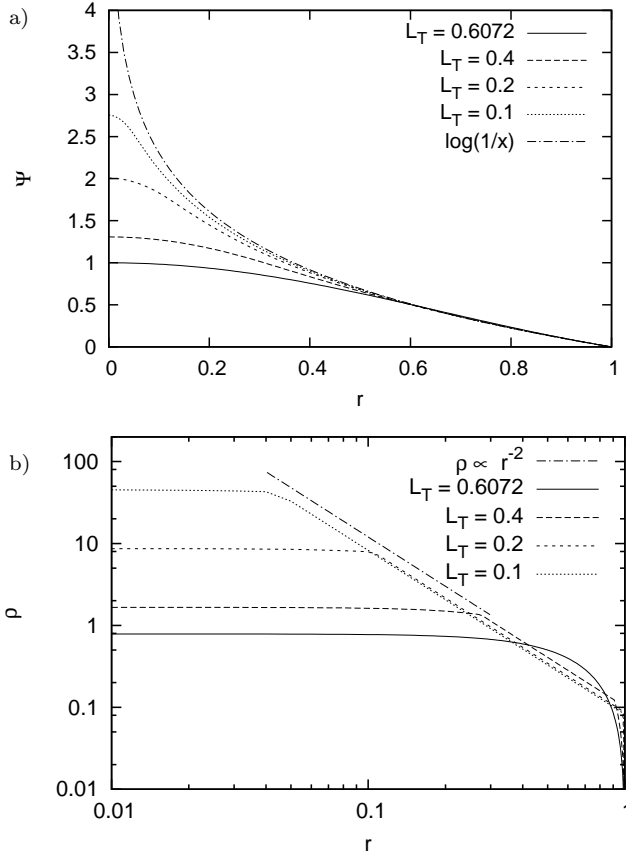


Figure 7. Same as in Fig. 6 for $q = -\frac{1}{2}$.

As it was discussed above, in general, there are three regions separated by radii r_1 and r_2 ($r_1 < r_2$). Taking into account boundary conditions (2.7), the potential can be written in the form

$$\Psi(r) = \begin{cases} \Psi_I(r) \equiv A \frac{\sin kr}{r}, & r < r_1, \\ \Psi_{II}(r) \equiv -N \ln r + C_1 + \frac{C_2}{r}, & r_1 < r < r_2, \\ \Psi_{III}(r) \equiv \frac{\sin[k(1-r)]}{kr}, & r_2 < r < 1, \end{cases}$$

where $k^2 = 2N/L_T^2$. To find six unknowns C_1 , C_2 , A , N , r_1 and r_2 there is a set of 6 algebraic equations: 4 conditions of continuity of the potential and its first derivative at points r_1 and r_2 , and 2 conditions (2.5) for determining the positions of r_1 and r_2 .

Table 1 gives the solutions of the model parameters for several values of L_T . Corresponding potential and density profiles are shown in Fig. 7. Note that in the purely radial model the density does not vanish on the boundary $r = 1$. In this case $\rho = 1/(4\pi r^2)$, $N = 1$, i.e., radial dependence of density is the same as that of the isothermal polytropic model.

4.4 Models with $q = -1$

In the limit $q \rightarrow -1$ the PPS polytropes turn into monoenergetic models

$$F(E, L_T) = \frac{N}{4\pi^3 L_T^2} H(L_T^2 - L^2) \delta(E), \quad (4.1)$$

L_T	N	r_1	r_2	A	C_1	C_2
0.6072	1.8194	0.6458	0.6458	0.3183	0.5817	-0.6039
0.4000	1.2784	0.2747	0.9102	0.3270	0.2218	-0.2235
0.2000	1.0854	0.1051	0.9795	0.2723	0.0743	-0.0744
0.1000	1.0325	0.0441	0.9950	0.1917	0.0299	-0.0299

Table 1. Solutions for the parameters of the potentials for $q = -\frac{1}{2}$ and several values of L_T .

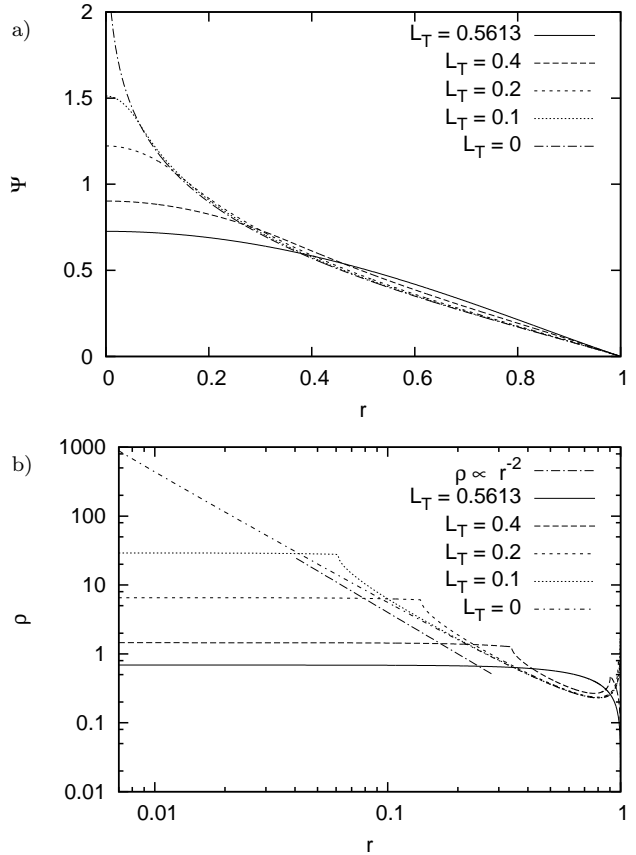


Figure 8. Same as in Fig. 6 for $q = -1$.

with density

$$\rho(r) = \frac{N}{\pi^2 L_T^2} (2\Psi)^{1/2} \mathcal{F}_{\frac{1}{2}}\left(\frac{L_T^2}{2r^2\Psi}\right). \quad (4.2)$$

Fig. 8 shows the profiles of the potential and density for $q = -1$ and several values of L_T . The potential profiles are monotonic for all values of parameter L_T . At $L_T = 0$ the potential has a central singularity $\Psi \propto [\ln(1/r)]^{2/3}$, in agreement with the earlier obtained expression (3.3) (see also Agekyan, 1962). On the contrary, density profiles appear to be non-monotonic, except for the case of isotropic model $L_T = L_{\text{iso}}$.

5 THE PRECESSION OF ORBITS

In this section we discuss precession of orbits and emphasize related problems that arise in systems with purely radial orbits with an example of models with $q = -\frac{1}{2}$. Such a choice is determined by the availability of an analytical expression for the potential for the purely radial system in this family, which is $\Psi = -\ln r$.

A star azimuth gains a rotation angle $\Delta\varphi$ during one radial period:

$$\Delta\varphi = 2L \int_{r_{\min}}^{r_{\max}} \frac{dr}{r^2 \sqrt{2(E - \ln r) - L^2/r^2}}.$$

Let $\alpha \equiv L/L_{\text{circ}}(E)$ be a ratio of the angular momentum L to the angular momentum of a star on the circular orbit with the same energy E , $L_{\text{circ}}(E) = \exp(E - \frac{1}{2})$. Changing the integration variable from r to $x \equiv r \exp(-E)$, we obtain (see also Touma and Tremain, 1997):

$$g(\alpha) \equiv \Delta\varphi = \frac{2\alpha}{\sqrt{e}} \int \frac{dx}{x \sqrt{-2x^2 \ln x - \alpha^2/e}}, \quad (5.1)$$

where $e = \exp(1)$. Note that in variables (E, α) the rotation angle is independent of energy. This is the case in all scale-free potentials such as $\Phi = K r^n$, or $\Phi = K \ln r$. The integration in (5.1) is over all x for which the radicand is positive. An explicit expression for function $g(\alpha)$ and its asymptotic expansion for nearly radial orbits can be obtained (using the Mellin transform). After some manipulations, one finally arrives at:

$$g(\alpha) = \pi + \frac{1}{\sqrt{\pi}} \text{p.v.} \int_0^\infty \alpha^t (2e)^{-t/2} \sin(\frac{1}{2} \pi t) t^{t/2-1} \Gamma(\frac{1}{2}(1-t)) dt,$$

where ‘p.v.’ stands for the principal value. Its asymptotic expansion at small α is:

$$g(\alpha) = \pi + \frac{1}{2} \pi \mu (1 + \frac{1}{2} \mu \ln 2\mu) + \mathcal{O}(\mu^3 \ln^2 \mu),$$

where

$$\mu = \frac{1}{\ln(1/\alpha)}.$$

The precession rate Ω_{pr} is expressed through $g(\alpha)$ using the relation:

$$\Omega_{\text{pr}} = \Omega_2 - \frac{1}{2} \Omega_1 = \frac{\Omega_1}{2\pi} [g(\alpha) - \pi],$$

where $\Omega_{1,2}(E, L)$ are radial and azimuthal frequencies

$$\frac{1}{\Omega_1} = \frac{1}{\pi} \int_{r_{\min}}^{r_{\max}} \frac{dr}{\sqrt{2E + 2\Psi(r) - L^2/r^2}},$$

$$\frac{\Omega_2}{\Omega_1} = \frac{L}{\pi} \int_{r_{\min}}^{r_{\max}} \frac{dr}{r^2 \sqrt{2E + 2\Psi(r) - L^2/r^2}},$$

For nearly radial orbits $\alpha \ll 1$, we have $\mu \ll 1$ and $\Omega_1(E, L) \approx \Omega_1(E, 0) = \sqrt{2/\pi} \exp(-E)$, so that the precession rate is

$$\Omega_{\text{pr}} \approx \frac{1}{\sqrt{8\pi}} \mu (1 + \frac{1}{2} \mu \ln 2\mu) e^{-E}.$$

The profiles $\Omega_{\text{pr}}(L)$ for several nearly radial systems

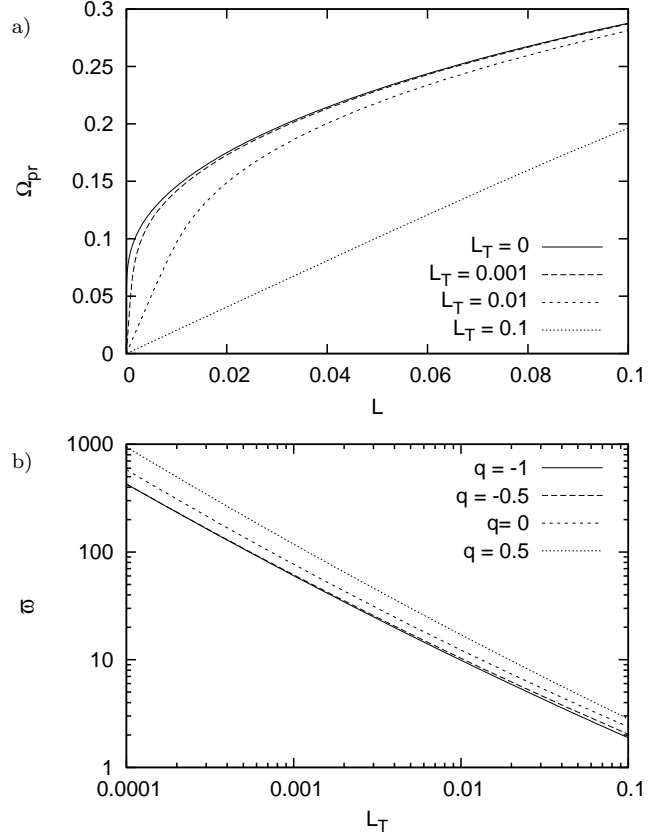


Figure 9. (a) Dependence of the precession rate $\Omega_{\text{pr}}(E = 0, L)$ for $q = -\frac{1}{2}$ and several values L_T for PPS polytropes. (b) Profiles of the precession rate slopes $\varpi(E = 0)$ v.s. parameter L_T for several values of q .

are shown in Fig. 9a. It is seen that precession rates depart quickly from zero at $L = 0$, and the slope is steeper for models with lower L_T . Thus, the derivative $\varpi(E) \equiv [\partial\Omega_{\text{pr}}/\partial L]_{L=0}$ tends to infinity as $L_T \rightarrow 0$.

This anomaly is quite typical for highly anisotropic models (including ones composed of purely radial orbits) in the class of GP, $F \propto (-2E)^q L^{-s}$. Since all of these models have gravitational force $\Psi' \propto r^{1-s}$ near the center (Hénon, 1973), it is singular for highly anisotropic DFs with $s > 1$. In Fig. 9b the profiles $\varpi(E)$ v.s. parameter L_T for different polytropic indices q are shown.

6 CONCLUSION

In this paper we proposed and studied two-parameter models of anisotropic spherical stellar systems. Dependence of DFs $F(E, L)$ on the energy E is adopted from the polytropic and generalized polytropic models. The dependence on the angular momentum is chosen in the form of the Heaviside function $H(L_T^2 - L^2)$, that allows only stars with the angular momenta $L < L_T$. For a given value of the polytropic index q , there is some critical value L_{iso} of L_T , above which the DFs are ergodic, and the systems are isotropic (see Fig. 10). The curve $L_T = L_{\text{iso}}(q)$ determines the upper boundary for the model parameters in (q, L_T) -plane.

The left and right boundaries of the permissible parameters coincide with the boundaries of the polytropic models. The left boundary is $q = -1$, where all stars have the same zero energy. The right boundary is a straight line $q = \frac{7}{2}$, where the models degenerate into the Plummer model and become isotropic for all values of L_T . There is no homogeneous model (one with the density independent of radius), because the corresponding value $q = -\frac{3}{2}$ is outside the permissible interval.

A natural lower boundary for possible model parameters is the horizontal axis $L_T = 0$. However, not all of the models with $L_T = 0$ are purely radial systems. Recall that purely radial models are models for which the global anisotropy parameter $\xi = 1$ (see (2.12)). Fig. 10a shows isolines $\xi(q, L_T) = \text{const}$ in the model's domain. The isotropic models correspond to $\xi(q, L_T) = 0$.

The most important feature of the proposed models is the existence of a wide region for parameter q , $-1 \leq q < \frac{1}{2}$, for which the limit $L_T = 0$ means the purely radial systems. This will enable us to use them in consistent analytic and numerical study of ROI, which cannot be performed correctly using systems with purely radial orbits only.

Outside this range, $q > \frac{1}{2}$, $L_T \rightarrow 0^+$ the potential degenerates into the Keplerian one, $\Psi(r) = 1/r - 1$, and models turn into points. We show that the global anisotropy $\xi(q, 0^+)$ varies linearly with polytropic index q (see (3.5)) from 1 to 0, which corresponds to transformation of models from purely radial to the isotropic ones.

Comparison of the parameter domains of PPS polytropes and GP is possible, recalling the relation $\xi = s/2$ for GP. In (q, s) -plane the boundary is a trapezoid with a vertical straight line $q = -1$, two horizontal straight lines $s = 0$ and $s = 2$ and a sloping side $2q + 3s = 7$ (Hénon 1973, Barnes, etc. 1986) or $2q + 6\xi = 7$ (see Fig. 10b). The straight line $s = 2$ corresponds to part of the boundary $q < \frac{1}{2}$, $L_T = 0$, and the sloping side corresponds to another part of x -axis: $q > \frac{1}{2}$, $L_T \rightarrow 0^+$. The right boundary of our model $q = \frac{7}{2}$ corresponds to single point $(q = \frac{7}{2}, s = 0)$ in the domain for the generalized polytropes (the Plummer model). Thus, the domain boundary for PPS polytropes coincide with the domain boundary of GP. This is not surprising, since if $q > \frac{1}{2}$, $L_T = 0^+$ the mass of the system is localized near the center. In fact, it means that sphere radius R tends to infinity. But just the same $R \rightarrow \infty$ occurs when reaching the boundary $2q = 3s = 7$ in GP (see Hénon 1973).

For a fixed L_T , central density concentration grows with increasing of the polytropic index q . For $q < -\frac{1}{2}$, the anisotropic models have intervals of growing density at the periphery of spheres. The Agekyan's model (1962) which is a particular case of our series at $q = -1$, $L_T = 0$, also has this feature.

For the model $q = -\frac{1}{2}$, we consider the precession rates at low angular momenta for nearly radial and purely radial orbits. Features of its behavior play a significant role for stability, first of all in the emergence of ROI (Polyachenko, etc. 2011). We have shown that in the limit of the purely radial systems, the derivative of the precession rate over L at $L = 0$ tends to infinity. This behavior is typical for all purely radial systems. Thus, the conventional methods of stability theory cannot be applied to study ROI in models

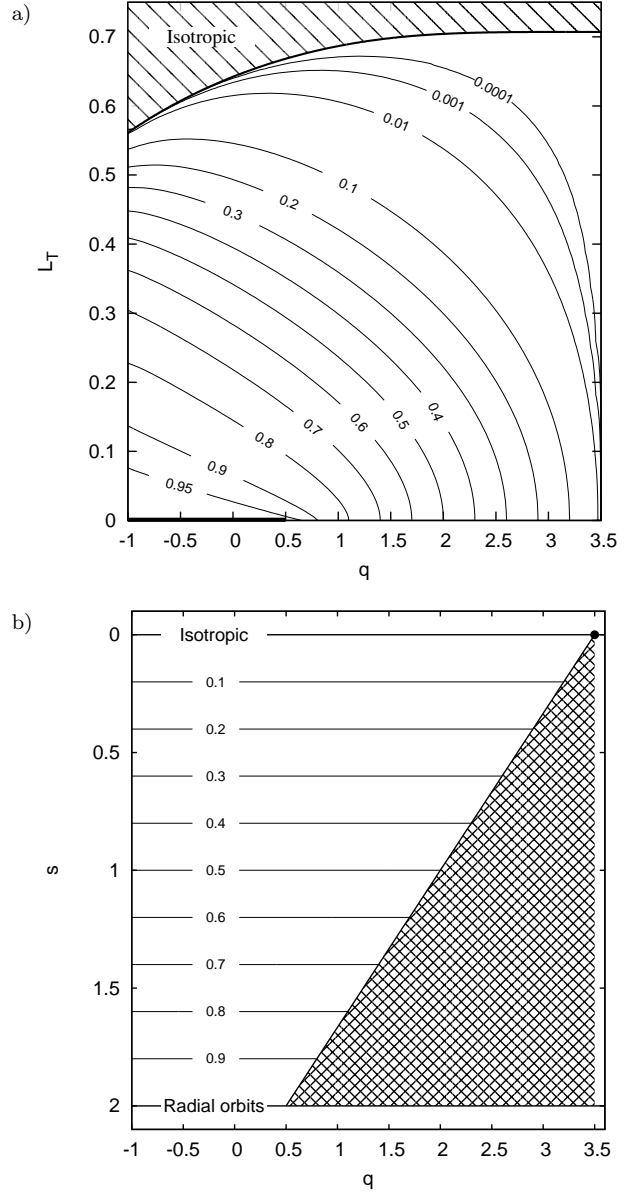


Figure 10. (a) Dependence of critical angular momentum $(L_T)_{\text{iso}}(q)$ (heavy line) and isolines of the global anisotropy ξ in the domain (q, L_T) of PPS polytropes. A part of the x -axis marked by a heavy line shows the models with purely radial orbits. (b) Domain of the parameters and isolines of anisotropy parameter ξ for GP.

with purely radial orbits. Suitable systems must have DFs with at least small but finite angular momentum dispersion.

Note that the generalized polytropes are also unsuitable for studying the instability by analytical methods (by solving the eigenvalue problem) because of the singular behavior of the density and the potential at $s \approx 2$.

In a separate work we shall present results of our study of ROI for families of models discussed above. The present work can be considered as the first step in this direction.

ACKNOWLEDGMENTS

The authors thank the referee for providing several valuable suggestions for presentation of the material, and Dr. Jimmy Philip for editing the original version of the article that helped to improve its quality. This work was supported by Sonderforschungsbereich SFB 881 'The Milky Way System' (subproject A6) of the German Research Foundation (DFG) and by Basic Research Program OFN-17 "The active processes in galactic and extragalactic objects" of Department of Physical Sciences of RAS.

REFERENCES

- Agekyan T. A., 1962, Vestnik Leningrad. Gos. Univ., Ser. math., mech., astr., No 1, 152 (in Russian)
 Antonov V. A., 1973, English translation in: de Zeeuw, T., ed. Proc. IAU Symp. 127, Structure and Dynamics of Elliptical Galaxies, Reidel, Dordrecht, p. 549
 Barnes J., Goodman J., Hut P., 1986, ApJ, 300, 112
 Binney J., Tremaine S., 2008, Galactic Dynamics: Second Edition. Princeton University Press, Princeton, NJ, USA
 Bisnovaty-Kogan G. S., Zel'dovich Ya. B., 1969, Astrofizika, 5, 425 (in Russian)
 Bouvier P., Janin G., 1968, Publ. Obs. Genève, A74, 186
 Chandrasekhar C., 1939, An introduction to the study of stellar structure. Dover publications, Inc.
 Dejonghe H., 1986, Phys. Rep., 133, 217
 Dejonghe H., Merritt D., 1992, ApJ, 391, 531
 Ernst A., Just A., 2013, MNRAS, 429, 2953
 Fridman A. M., Polyachenko V. L., 1984, Physics of Gravitating Systems. Springer, New York
 Gelfand I. M., Shilov G. E., 1964, Generalized functions. Academic Press, Inc.
 Hénon M., 1973, A&A, 24, 229
 Kharchenko, N. V., Berczik, P., Petrov, M. I., Piskunov, A. E., Röser, S., Schilbach, E., 2009, A&A 495, 807
 Merritt D., 1985, AJ, 90, 1027
 Osipkov L. P., 1979, Soviet Astron. Lett. 5, 42
 Palmer P. L., 1994, Stability of collisionless stellar systems: mechanisms for the dynamical structure of galaxies. Astrophysics and Space Science Library, Kluwer, Dordrecht, Boston
 Polyachenko V. L., Polyachenko E. V., Shukhman I. G., 2010, Astron. Lett., 36, 175
 Polyachenko E. V., Polyachenko V. L., Shukhman I. G., 2011, MNRAS, 416, 1836
 Richstone D., Tremaine S., 1984, ApJ, 286, 27
 Touma J., Tremaine S., 1997, MNRAS, 292, 909

APPENDIX. Approximate analytical solution for model $q = \frac{1}{2}$ with almost radial orbits, $L_T \ll 1$

We saw in Sec. 3 that for $q \geq \frac{1}{2}$ there are no models with purely radial orbits. Now we construct a physically appropriate solution on the boundary $q = \frac{1}{2}$ for arbitrary small

but finite L_T . From (2.3) and (2.6) one obtains:

$$\Psi'' + \frac{2}{r} \Psi' = -3N \begin{cases} \frac{\Psi^2}{L_T^2} & \text{for } 0 < r < r_1, \\ \frac{\Psi}{r^2} - \frac{L_T^2}{4r^4} & \text{for } r_1 < r < 1. \end{cases} \quad (\text{A1})$$

In the above equation, r_1 defined by $L_T^2 = 2r_1^2\Psi(r_1)$ separates two regions, I and II. In general, there is a region III adjacent to the sphere boundary (see Sec. 2), but for small L_T it can be ignored since its width is of the order of L_T^2 . Equation (A1) is to be solved with boundary conditions

$$\Psi(1; L_T, N) = 0, \quad \Psi'(1; L_T, N) = -1, \quad \Psi'(0; L_T, N) = 0.$$

In region II (A1) is a inhomogeneous linear equation. The solution satisfying the boundary conditions at the right boundary $r = 1$ is

$$\Psi_{II}(r) = \frac{1 + 4\nu^2}{9 + 4\nu^2} \frac{L_T^2}{4} \left[\frac{1}{r^2} - \frac{3}{2\nu\sqrt{r}} \sin\left(\nu \ln \frac{1}{r}\right) - \frac{1}{\nu\sqrt{r}} \cos\left(\nu \ln \frac{1}{r}\right) \right] + \frac{1}{\sqrt{r}} \sin\left(\nu \ln \frac{1}{r}\right), \quad (\text{A2})$$

where $\nu = \sqrt{3N - \frac{1}{4}}$ is a *real* parameter. Taking into account that for $L_T \ll 1$ radius r_1 is also very small, $r_1 \ll 1$, and ignoring trigonometric terms in square brackets in (A2), we obtain

$$L_T^2 = 4r_1^{3/2} \frac{\sin(\nu\Lambda_1)}{\nu} \frac{9 + 4\nu^2}{17 + 4\nu^2}, \quad \Lambda_1 \equiv \ln \frac{1}{r_1}, \quad (\text{A3})$$

$$\Psi_{II}(r_1) = \frac{2(9 + 4\nu^2)}{17 + 4\nu^2} \frac{\sin(\nu\Lambda_1)}{\nu\sqrt{r_1}}. \quad (\text{A4})$$

Since the function $\Psi(r)$ is positive, the condition $\nu\Lambda_1 < \pi$ must be satisfied.

In the region I (A1) can be written using new independent variable $x \equiv r/r_1$:

$$\frac{1}{x^2} \frac{d}{dx} x^2 \frac{d\Theta}{dx} = -\frac{3}{2} N \Theta^2 \equiv -\frac{1}{8} (1 + 4\nu^2) \Theta^2, \quad (\text{A5})$$

where $\Theta(x) \equiv \Psi_I(r_1 x)/\Psi_I(1)$ is a new unknown function. The boundary conditions to be satisfied are:

$$\Theta'(0) = 0, \quad \Theta(1) = 1,$$

$$\Theta'(1) = -\frac{21 + 20\nu^2}{4(9 + 4\nu^2)} - \frac{\nu(17 + 4\nu^2)}{2(9 + 4\nu^2)} \cot(\nu\Lambda_1). \quad (\text{A6})$$

The expression for $\Theta'(1)$ follows from the continuity of the first derivative of the potential at $r = r_1$. Equation (A6) with boundary conditions (A7) can be solved numerically using standard shooting method for $\nu_1 \equiv \nu(\Lambda_1)$, where Λ_1 is considered as a control parameter. Then the relation $\nu = \nu(L_T)$ (and also $3N(L_T) = \nu^2(L_T) + \frac{1}{4}$) is obtained from the equality which follows straightforwardly from (A3):

$$L_T = 2 \exp\left(-\frac{3}{4} \Lambda_1\right) \sqrt{\frac{\sin(\nu_1 \Lambda_1)}{\nu_1} \frac{9 + 4\nu_1^2}{17 + 4\nu_1^2}}, \quad (\text{A7})$$

The dependence of the tripled normalization constant N for small L_T is shown in Fig. 11. (Recall that for $q = \frac{1}{2}$ we have $(L_T)_{\text{iso}}(\frac{1}{2}) = 0.6682$ and $3N((L_T)_{\text{iso}}) = 4.686$.) It was useful to start the shooting procedure from $\Lambda_1 \simeq 30$ which implies

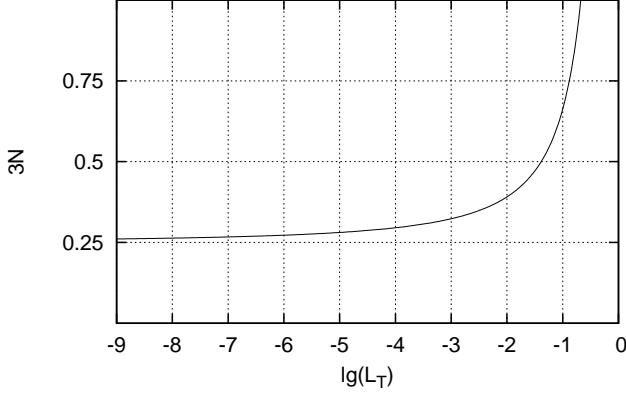


Figure 11. The tripled normalization constant $N(L_T)$ for models with $q = 1/2$ and small L_T .

very small r_1 and $3N - \frac{1}{4} \ll 1$. For large Λ_1 , one can find an asymptotic expansion for ν by applying perturbation theory to (A6) and using factor $\frac{1}{8}$ in the r.h.s. as a small parameter:

$$\nu \approx \frac{\pi}{\Lambda_1} - \kappa \frac{\pi}{\Lambda_1^2}, \quad (\text{A8})$$

where $\kappa = 68/39$. Note that from (A8) and (A3) it follows that

$$\frac{\sin(\nu\Lambda_1)}{\nu} \approx \kappa, \quad L_T^2 \approx \frac{36}{17} \kappa r_1^{3/2} = \mathcal{O}(r_1^{3/2}),$$

i.e., $r_1 = \mathcal{O}(L_T^{4/3})$, that justifies omitting trigonometric contributions of order L_T^2 in derivation of (A3). For potential in the center we have an estimate

$$\Psi(0) \approx \frac{49}{96} \left(\frac{36}{17} \kappa \right)^{4/3} L_T^{-2/3} = 2.91 L_T^{-2/3}.$$

This analytical solution shows that the potential become singular with $L_T \rightarrow 0$, but is remains regular as long as L_T is arbitrary small, but finite.